Dynamic Feedback based Adaptive Modulation for Energy-efficient Communication

Priyadarshi Mukherjee and Swades De

Abstract—Conventional adaptive modulation (AM) scheme achieves capacity gain by adapting its modulation index with the wireless channel state. The channel state information (CSI) is learned from receiver feedback in every time slot, which wastes energy. In this work, we propose to exploit temporally-correlated dynamic wireless channel state to compute CSI-dependent interval between successive feedback and select an appropriate modulation index in AM-based transmission. Our analysis and numerical results demonstrate that the proposed dynamic feedback-based AM offers about 22% or higher energy efficiency along with 13% or higher data throughput over its nearest competitive approach in nominal mobility range.

Index Terms—Adaptive modulation, fading channel, dynamic feedback, energy efficiency

I. INTRODUCTION

Adaptive modulation (AM) [1] is a prevalent physical layer technique for achieving high throughput over wireless channels. In AM, the transmitter (Tx) adapts its modulation scheme according to channel conditions. When the channel is in deep fade, Tx does not send any data payload.

It was shown in [2] that AM enhances spectral efficiency while maintaining a target error performance over fading channel. Here, Tx requires regular channel state information (CSI) feedback from the receiver (Rx), resulting in energy waste. The authors in [3] proposed a variant of AM, which reduces chances of blind transmission when the channel is in deep fade. However, as in [2], this variant also requires regular CSI feedback. In context of avoiding regular CSI feedback, there exist some channel-dependent transmission strategies [4], [5] that exploit temporal correlation in channel to decide on transmission and waiting windows. However, [4], [5] do not involve channel dependent variation of modulation scheme.

In view of feedback related energy efficiency, we investigate the role of temporally-correlated wireless channel on AM. We propose to extend the interval between consecutive CSI feedbacks. An analytical framework is developed to estimate the duration over which the channel state is expected to remain within two thresholds neighboring the current signal level. We incorporate this information in our proposed dynamic feedback-based AM (DF-AM) for improved energy efficiency. Though DF-AM incurs a little additional overhead for conveying the estimated interval to Rx, numerical results show that, it offers at least 22% energy efficiency and an overall 13% or higher data throughput over the closest competitive approach.

II. SYSTEM MODEL AND PROTOCOL DESCRIPTION

System Model: An AM-based point-to-point wireless communication is considered. General assumptions are: slotted communication with slot duration T_s; data frames are always available for transmission; the channel remains invariant in a frame duration T_f but may vary from frame to frame [2].

Based on received signal quality, Rx sends useful CSI, such as channel state estimate X_0 and maximum Doppler frequency f_D. f_D corresponding to relative velocity v of Rx is $f_D \cong \frac{v f_c}{c}$, where f_c is the carrier frequency and c is the velocity of light in vacuum. The product $f_D T_s$ characterizes the temporally varying wireless channel [6]; $f_D T_s > 0.2$ indicates an almost independent 'fast' fading channel, whereas $f_D T_s < 0.1$ implies a correlated 'slow' fading one.

The entire X range is partitioned into intervals with thresholds $\{X_{T_i}\}_{i=0}^{I}$, where each interval corresponds to a modulation level i. Thresholds $\{X_{T_i}\}_{i=0}^{I}$ are determined based on the required bit error rate P_b as [7]:

$$P_b = a_1 \exp\left(\frac{-a_2 X_0^2}{N_0 B(i^{a_3} - a_4)}\right). \tag{1}$$

Here $a_1, \cdots, a_4$ are modulation-specific constants, N_0 is the noise spectral density, and B is the channel bandwidth.

Protocol Description: The unique features of the proposed DF-AM protocol are: (i) Based on the CSI feedback level X_0, Tx estimates the duration $\theta_{i,i+1}$ over which the channel state X is expected to remain in $\left[X_{T_i}, X_{T_{i+1}}\right)$, when $X_0 \in \left[X_{T_i}, X_{T_{i+1}}\right)$. (ii) Tx communicates this $\theta_{i,i+1}$ information to Rx. (iii) Data frames are transmitted over this duration with AM index i, and a feedback is sent from Rx at the end of this duration, which also contains CSI for determining the next cycle of $\theta_{i,i+1}$. (iv) The feedback contains information of the erroneously received data packets. (iv) Before transmission of new data frames in a cycle, the erroneously delivered frames are retransmitted. (v) If $X_0 \in [X_{T_0}, X_{T_1})$, Tx does not transmit any data; it waits for the estimated $\theta_{0,1}$ before sending a probing packet and re-estimates $\theta_{i,i+1}$ based on feedback.

Note that, unlike in [1]–[3], DF-AM requires feedback once in $\theta_{i,i+1}$, as it aims to reduce feedback frequency and energy consumption by exploiting CSI. We also observe that the proposed framework can be extended to include coded modulation schemes using the coding gain model in [7, Section 9.3.8].

III. ANALYTICAL FRAMEWORK

If the signal envelope at Rx is $X(t) = \sqrt{P}|h|$, its probability distribution $f_X(x)$ depends on the underlying fading model. However, time derivative of $X(t)$, i.e., $\dot{X}(t) \triangleq \frac{dX(t)}{dt}$ is a zero mean Gaussian random variable (RV) irrespective of $f_X(x)$,

i.e., $\dot{X}(t) \sim \mathcal{N}(0, \dot{\sigma})$ [8]. Using this interesting property of $\dot{X}$ (index t is removed for brevity), we estimate the probability of $X(t)$ staying in $\left[X_{T_i}, X_{T_{i+1}}\right)$, given that $X_0 \in \left[X_{T_i}, X_{T_{i+1}}\right)$.

As $\theta_{i,i+1}$ estimation depends on $\dot{X}(t)$, the proposed framework is generic and independent of the underlying $f_X(x)$.

A. Distribution of Temporal Variation of Channel State

Let us assume $X(t) = X_0$ and $X_0 \in \left[X_{T_i}, X_{T_{i+1}}\right)$. X in next time slot can be obtained by Taylor series expansion as:

$$X(t + T_s) = X(t) + \dot{X} \cdot T_s + \ddot{X} \cdot \frac{T_s^2}{2!} + \cdots$$
$$\approx X(t) + \dot{X} \cdot T_s \quad (\because T_s \ll 1) \qquad (2)$$

Probability that X will remain in $\left[X_{T_i}, X_{T_{i+1}}\right)$ in next slot is

$$\Pr\left\{X_{T_i} \le X(t + T_s) < X_{T_{i+1}}\right\}$$
$$\overset{\text{by (2)}}{\approx} \Pr\left\{X_{T_i} \le X_0 + X_1 < X_{T_{i+1}}\right\}. \quad (3)$$

Here $X_1 \left(= \dot{X} \cdot T_s\right)$ is a RV that denotes temporal variation of X in the next slot. Hence we have $X_1 \sim \mathcal{N}(0, \dot{\sigma}_1)$ where $\dot{\sigma}_1 = T_s \dot{\sigma}$. X_1 being a Gaussian RV, $X_1 \in (-\infty, \infty)$. On the other hand, X is the signal envelope, i.e., $X_1 \in [-X_0, \infty)$. Therefore, X_1 follows a truncated Gaussian distribution:

$$f_{X_1}(\alpha) = \begin{cases} \frac{1}{1 - \Phi_1\left(-\frac{X_0}{\dot{\sigma}_1}\right)} \frac{1}{\sqrt{2\pi}\dot{\sigma}_1} e^{\left(\frac{-\alpha^2}{2\dot{\sigma}_1^2}\right)} & -X_0 \le \alpha \\ 0 & \text{elsewhere.} \end{cases} \quad (4)$$

Here $\Phi_1(x) = \int_{-\infty}^{x} \frac{1}{\sqrt{2\pi}} e^{-\frac{t^2}{2}} dt$ is the cumulative distribution function (CDF) of standard univariate normal distribution and $\dot{\sigma}_1$ depends on the underlying fading model. Using (4) in (3),

$$\Pr\left\{X_{T_i} \le X_0 + X_1 < X_{T_{i+1}}\right\}$$
$$= \int_{X_{T_i}-X_0}^{X_{T_{i+1}}-X_0} f_{X_1}(\alpha)d\alpha = \frac{\Phi_1\left(\frac{X_{T_{i+1}}-X_0}{\dot{\sigma}_1}\right) - \Phi_1\left(\frac{X_{T_i}-X_0}{\dot{\sigma}_1}\right)}{1 - \Phi_1\left(-\frac{X_0}{\dot{\sigma}_1}\right)}. \quad (5)$$

Similarly, probability that X will continue to remain in $\left[X_{T_i}, X_{T_{i+1}}\right)$ for next ζ slots is:

$$\Pr\left\{X_{T_i} \le X(t + T_s) < X_{T_{i+1}}, \cdots, \right.$$
$$\left. X_{T_i} \le X(t + \zeta T_s) < X_{T_{i+1}}\right\}$$
$$\overset{\text{by (3)}}{\approx} \Pr\left\{X_{T_i} \le X_0 + X_1 < X_{T_{i+1}}, \cdots, \right.$$
$$\left. X_{T_i} \le X_0 + X_\zeta < X_{T_{i+1}}\right\}. \quad (6)$$

Like X_1, X_ζ is zero mean truncated Gaussian with $\dot{\sigma}_\zeta^2 = \zeta\dot{\sigma}_1^2$. In general $X_1, \cdots, X_\zeta$ are not independent. Thus (6) becomes:

$$\Pr\left\{X_{T_i} \le X_0 + X_1 < X_{T_{i+1}}, \cdots, X_{T_i} \le X_0 + X_\zeta < X_{T_{i+1}}\right\}$$
$$= \int_{X_{T_i}-X_0}^{X_{T_{i+1}}-X_0} \cdots \int_{X_{T_i}-X_0}^{X_{T_{i+1}}-X_0} f_{\underline{X_\zeta}}(\underline{x_\zeta}, \Sigma, \underline{X_{\zeta 0}})d\underline{x_\zeta}. \quad (7)$$

$f_{\underline{X_\zeta}}(\underline{x_\zeta}, \Sigma, \underline{X_{\zeta 0}})$ is ζ-variate truncated Gaussian, given by [9]:

$$f_{\underline{X_\zeta}}(\underline{x_\zeta}, \Sigma, \underline{X_{\zeta 0}}) = \frac{e^{-\frac{1}{2}\underline{x_\zeta}^T \Sigma^{-1} \underline{x_\zeta}}}{\int_{\underline{X_{\zeta 0}}}^{\infty} e^{-\frac{1}{2}\underline{x_\zeta}^T \Sigma^{-1} \underline{x_\zeta}} d\underline{x_\zeta}}; \quad \underline{x_\zeta} \in \mathbb{R}^\zeta_{\ge \underline{X_{\zeta 0}}}.$$

Here $\underline{X_\zeta} = [X_1, \cdots, X_\zeta]^T$ is a ζ-dimensional RV, Σ is the $\zeta \times \zeta$ positive definite covariance matrix of $\underline{X_\zeta}$, $\underline{X_{\zeta 0}} = -X_0\underbrace{[1, \cdots, 1]}_{\zeta \text{ times}}^T$, $\mathbb{R}^\zeta_{\ge \underline{X_{\zeta 0}}} = \left\{\underline{x_\zeta} \in \mathbb{R}^\zeta : \underline{x_\zeta} \ge \underline{X_{\zeta 0}}\right\}$, and $\int_{\underline{X_{\zeta 0}}}^{\infty}$ is an ζ-dimensional Riemann integral from $\underline{X_{\zeta 0}}$ to ∞. The integral in (7) is solved using the algorithm proposed in [10] for multivariate Gaussian probability computations.

B. Duration of Stay (DoS) Estimation

(6) can be interpreted as, X will 'cross-over' $\left[X_{T_i}, X_{T_{i+1}}\right)$ within these ζ slots with a probability of $\epsilon(\zeta)$, where

$$\epsilon(\zeta) = 1 - \Pr\left\{X_{T_i} \le X_0 + X_1 < X_{T_{i+1}}, \cdots, \right.$$
$$\left. X_{T_i} \le X_0 + X_\zeta < X_{T_{i+1}}\right\}. \quad (8)$$

We now estimate the *DoS* of X in $\left[X_{T_i}, X_{T_{i+1}}\right)$. It gives a measure of time over which $X \in \left[X_{T_i}, X_{T_{i+1}}\right)$ given that $X_0 \in \left[X_{T_i}, X_{T_{i+1}}\right)$. If DoS$= \zeta$ slots, then $\theta_{i,i+1} = \zeta T_s$ sec.

We calculate ζ^* (optimal value of ζ) for a given set of system parameters (f_D and T_s), X_0, X_{T_i}, $X_{T_{i+1}}$, and ϵ_0(user-defined ϵ) by solving the following optimization problem P1:

$$\text{(P1)} \quad : \underset{\zeta \ge 0}{\text{maximize}} \ \zeta \quad \text{subject to} \quad \epsilon(\zeta) \le \epsilon_0, \quad (9)$$

where $\epsilon(\zeta)$ is calculated according to (8). We observe from P1 that obtaining ζ^* involves sequential search method with ζ starting from 1. Moreover, the search is also accompanied by integration over ζ-variate truncated Gaussian distributions in each step. Hence we propose a lower bound ζ_l of ζ to reduce the search space, which leads to obtaining ζ^* in considerably less time. Accordingly we reformulate P1 to P3 (with $\zeta \ge \zeta_l$):

$$\text{(P2)} \quad : \underset{\zeta \ge \zeta_l}{\text{maximize}} \ \zeta \quad \text{subject to} \quad \epsilon(\zeta) \le \epsilon_0. \quad (10)$$

ζ_l is computed considering independence among the X_i's, i.e.,

$$\Pr\left\{X_{T_i} \le X_0 + X_1 < X_{T_{i+1}}, \cdots, X_{T_i} \le X_0 + X_\zeta < X_{T_{i+1}}\right\}$$
$$= \prod_{p=1}^{\zeta} \Pr\left\{X_{T_i} \le X_0 + X_p < X_{T_{i+1}}\right\}$$
$$= \prod_{p=1}^{\zeta} \frac{\Phi_1\left(\frac{X_{T_{i+1}}-X_0}{\dot{\sigma}_p}\right) - \Phi_1\left(\frac{X_{T_i}-X_0}{\dot{\sigma}_p}\right)}{1 - \Phi_1\left(-\frac{X_0}{\dot{\sigma}_p}\right)}, \quad (11)$$

where X_p is a zero mean truncated Gaussian RV with $\sigma_p^2 = p\sigma_1^2$. We accordingly obtain ζ_l as:

$$\text{(P2)} \quad : \underset{\zeta \ge 0}{\text{maximize}} \ \zeta \quad (12)$$

$$\text{subject to} \quad \prod_{p=1}^{\zeta} \frac{\Phi_1\left(\frac{X_{T_{i+1}}-X_0}{\dot{\sigma}_p}\right) - \Phi_1\left(\frac{X_{T_i}-X_0}{\dot{\sigma}_p}\right)}{1 - \Phi_1\left(-\frac{X_0}{\dot{\sigma}_p}\right)} \ge 1 - \epsilon_0.$$

Note that, unlike P1, P2 does not require computation of multivariate Gaussian probabilities. Later in Section V we discuss the importance of the proposed lower bound ζ_l.

IV. PERFORMANCE EVALUATION OF DF-AM

Data frames are assumed to be of single slot size, i.e., $T_f = T_s$. Feedback and probing packets are assumed very small compared to T_s, i.e., $T_{fp} = \gamma T_s (\gamma \ll 1)$ [5]. Performance of DF-AM is measured in terms of the following metrics:

A. Data throughput $\mathcal{R}_\mathcal{D}$

$\mathcal{R}_\mathcal{D}$ is the long-term average of data transmissions rate, i.e.,

$$\mathcal{R}_\mathcal{D} = \lim_{K \to \infty} \frac{(1 - \epsilon_0) \sum_{k=1}^{K} \zeta(k) R_i(k)[1 - P_b(k)]}{\sum_{k=1}^{K} \{\theta_{i,i+1}(k) + 2T_{fp}\}}. \quad (13)$$

Here $R_i(k)[1 - P_b(k)]$ is the data rate with modulation level i [2], and $2T_{fp}$ accounts for the two-way Rx-Tx handshake.

B. Energy efficiency η

Throughput and energy trade-off is captured by energy efficiency $\eta = \dfrac{\mathcal{R}_\mathcal{D}}{\mathcal{E}_\mathcal{C}}$; $\mathcal{E}_\mathcal{C}$ is per-slot energy consumption, i.e.,

$$\mathcal{E}_\mathcal{C} = \lim_{K \to \infty} \frac{\sum_{k=1}^{K} e_c(k)}{\sum_{k=1}^{K} \zeta(k)}, \quad (14)$$

where $e_c(k) = [\theta_{i,i+1}(k)\mathcal{P}_{ps} + \mathcal{P}_p T_{fp}] \mathbb{1}_{\{i=0\}} + \mathcal{P}_r T_{fp} + \theta_{i,i+1}(k)\mathcal{P}_t \mathbb{1}_{\{i \neq 0\}}$. $\mathbb{1}_{\{x\}}$ is an indicator function that takes 1 when x holds, and 0 otherwise.

$\mathbb{1}_{\{i=0\}}$ in (14) implies that, when the channel is in deep fade, Tx estimates $\theta_{0,1}$ to enter the power-saving mode. Tx sends a probing signal after $\theta_{0,1}$ to re-estimate $\theta_{i,i+1}$ depending on the feedback, and accordingly decide on the modulation level i. $\mathcal{P}_t$(respectively, $\mathcal{P}_r$) denotes transmit (respectively, receive) power, $\mathcal{P}_{ps}$ is the power dissipated in power-saving mode, and $\mathcal{P}_p$ is the probing signal power consumption. It may be noted that, both $\mathcal{R}_\mathcal{D}$ and $\mathcal{E}_\mathcal{C}$ being functions of the user-defined ϵ_0, η is also a function of ϵ_0.

V. NUMERICAL RESULTS AND DISCUSSIONS

We present numerical results to evaluate the performance of DF-AM. Results are obtained over a Rayleigh fading channel. System parameters are: carrier frequency $f_c = 900$ MHz, $T_s = 100$ μs, and $\gamma = 0.1$. Power consumption: $\mathcal{P}_t, \mathcal{P}_p = 60$ mW, $\mathcal{P}_r = 45$ mW, and $\mathcal{P}_{ps} = 18$ mW [11]. As M-QAM is employed at Tx, from (1) we have $P_b = 2\exp\left(\frac{-1.5X_0^2}{N_0 B(i-1)}\right)$ [7]. Using $P_b = 10^{-3}$ [2] and $N_0 B = 1$, we illustrate our claim over the following transmission modes (TM):

A. Verification of Analysis

Fig. 1 shows that $\theta_{i,i+1}$ matches closely with simulation results. As observed, X_0 plays a significant role in estimating $\theta_{i,i+1}$. Note that irrespective of v, $\theta_{i,i+1}$ is comparatively lesser when X_0 is closer to a X_{T_i} $\forall$ i, i.e., $\theta_{i,i+1}(6.5), \theta_{i,i+1}(9.5)$, and $\theta_{i,i+1}(14)$ are lesser than their

Table I. Transmission Modes.

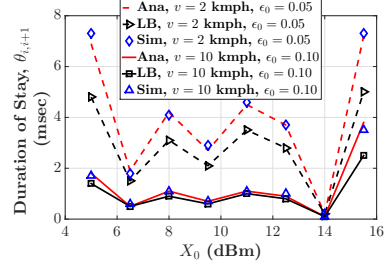| X_T (dBm)	Modulation	R_i (bits/sym.)
$X_0 < 6.9897$	No transmission	0
$6.9897 \leq X_0 < 10.0000$	BPSK	1
$10.0000 \leq X_0 < 11.7609$	QPSK	2
$11.7609 \leq X_0 < 13.0103$	8-QAM	3
$13.0103 \leq X_0 < 13.9794$	16-QAM	4
$13.9794 \leq X_0 < 14.7712$	32-QAM	5
$14.7712 \leq X_0$	64-QAM	6

Fig. 1. Verification of DoS estimation via Monte Carlo simulation. 'Ana': Analytical; 'LB': Lower bound; 'Sim': Simulation.

immediate neighbors. This is intuitive also; X_0 nearer to a threshold takes lesser time to cross it than otherwise.

Fig. 1 also demonstrates the variation of estimated lower bound $\theta_{i,i+1}^l (= \zeta_l T_s$ sec). We observe that there exists a considerable gap between $\theta_{i,i+1}^l$ and $\theta_{i,i+1}$ at lower v, but they almost converge with increasing v. The reason being that $\theta_{i,i+1}^l$ is calculated assuming complete independence but the channel is highly correlated at lower v. With increasing v, the channel is less correlated and hence resulting in merging of the two. This also illustrates the importance of $\theta_{i,i+1}^l$, especially when the channel is varying very slowly; it considerably reduces the search space for estimating $\theta_{i,i+1}$.

Remark. *'Average fade region duration' (AFRD) [7] defines the average time that X stays within $\left[X_{T_i}, X_{T_{i+1}}\right) \forall i$. It does not consider the current state X_0. Fig. 1 demonstrates the importance of X_0, which unlike AFRD, is taken into account by the proposed DoS estimation scheme.*

B. Margin of Error

It is difficult to estimate the time-varying channel behavior. Hence we calculate $\theta_{i,i+1}$ with an acceptable error margin Δ^{err}, where $\Delta^{\text{err}} = R^{\text{act}} - R^{\text{est}}$; R^{act} and R^{est} denote the rate of actual and estimated TM in i^{th} slot. Hence, (i) $\Delta^{\text{err}} = 0$: correct choice of TM. (ii) $\Delta^{\text{err}} > 0$: under-utilization of channel, i.e., TM used in DF-AM is lower than the current capability. (iii) $\Delta^{\text{err}} < 0$: over-utilization of channel, i.e., channel is not suitable of using higher TM but DF-AM does so.

Fig. 2(a) captures the variation of Δ^{err} over an interval of 1000 slots. It also compares the accuracy of DF-AM with coherence time $t_{\text{ch}} = \frac{0.423}{f_D}$ [12]-based transmission scheme, where TM is updated once in t_{ch}. We observe that $\Delta^{\text{err}} \neq 0$ over $\sim 10\%$ of transmission slots in DF-AM, whereas it is $\sim 60\%$ in t_{ch}-based scheme. This highlights the efficiency of channel utilization with DF-AM. This figure also reaffirms the claim in [13], i.e., the concept of t_{ch} is good for systems
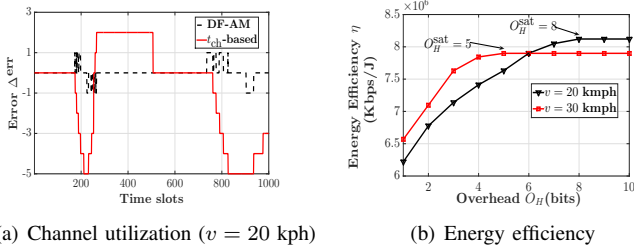
(a) Channel utilization ($v = 20$ kph) (b) Energy efficiency

Fig. 2. Resource utilization performance of DF-AM. $\epsilon_0 = 0.05$.

(a) Data throughput (b) Energy efficiency.

Fig. 3. Performance comparison of our proposed DF-AM. $\epsilon_0 = 0.05$.

that focus on average performance. However, in scenarios where worst-case performance guarantee is required, such as in ultra-reliable low-latency communications, t_{ch}-based channel estimate falls short, instead DF-AM will be more effective.

C. Overhead

In DF-AM, Tx estimates $\theta_{i,i+1}$ and communicates it to Rx. To do so, it requires an overhead of O_H bits. Probing into the role of O_H on the efficiency of DF-AM, we obtain Fig. 2(b), where we vary η against O_H. We observe that η initially increases and saturates beyond a certain O_H^{sat}.

Observe that O_H^{sat} at $v = 20$ kph is higher than $v = 30$ kph. This fact corroborates the claim from Fig 1, i.e., for identical X_0, $v_1 < v_2$ implies $\theta_{i,i+1}$ for $v = v_1$ is more than $\theta_{i,i+1}$ for $v = v_2$ due to the higher correlation in channel. Hence more bits are required to convey this information to Rx. Note that DF-AM requires this overhead once in $\theta_{i,i+1}$ and unlike AM, avoids regular CSI feedback from Rx. Lastly, Fig. 2(b) suggests that $O_H = 8$ bits can be safely considered, as higher values do not provide any additional benefit.

D. Relative Performance

The competitive approaches are:
(i) AM [2]: This is the classical approach, i.e., adjust the TM in each time slot based on the feedback from Rx.
(ii) FD [3]: It estimates only $\theta_{0,1}$ if $X_0 \in [X_{T_0}, X_{T_1})$ and requires regular feedback otherwise. It proposed $\theta_{0,1} = \left\lceil \frac{0.5 \times (\rho_{X_{T_0}} - \rho_{X_0})}{T_s} \right\rceil$, where $\rho_{X_{\text{th}}}$ is the *average fade duration* (AFD) for a threshold X_{th} [7]: $\rho_{X_{\text{th}}} = \frac{\Pr\{X < X_{\text{th}}\}}{\int_0^\infty \dot{x} f_{X, \dot{X}}(X_{\text{th}}, \dot{x}) d\dot{x}}$.
(iii) Dynamic window transmission (DW) [5]: It decides both the transmission and waiting window depending on X_0. However, it does not change TM during data transmission and always uses a fixed TM. Here we assume that QPSK is employed whenever transmission takes place.

Now we compare DF-AM against these schemes.

A) Data Throughput $\mathcal{R}_D$: Fig. 3(a) demonstrates an overall decreasing trend of $\mathcal{R}_D$. This is because increasing v results in high $f_D T_s$ product, i.e., the channel is now less correlated than it was with lower $f_D T_s$. This results in lower DoS ζ for the same X_0, which implies decrease of both $\mathcal{R}_D$ and η.

We observe that $\mathcal{R}_D$ of DW, AM, and FD are considerably lesser compared to DF-AM. This is because DW intelligently estimates the transmission and waiting intervals; but it does
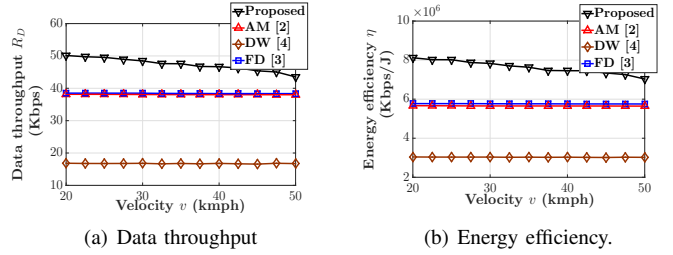
not alter TM depending on X_0. AM does not apply any intelligence in terms of avoiding regular CSI feedback, whereas FD only estimates $\theta_{0,1}$ if $X_0 \in [X_{T_0}, X_{T_1})$. On the other hand, DF-AM decides on both TM and duration $\theta_{i,i+1}$. This results in a considerable $\mathcal{R}_D$ gain in the range of $13\% - 31\%$ with respect to its nearest approach, depending on the node mobility. In addition to this gain, the main advantage of DF-AM is its high energy efficiency, which is discussed next.

B) Energy Efficiency η:: The energy consumption parameters are taken from Microchip ATZB-900-B0R data sheet [11]. It can be seen from 3(b) that the DF-AM consistently achieves higher η with respect to its nearest benchmark scheme, which is around $22\% - 40\%$, depending on the node mobility. Note that, as in Fig. 3(a), here also we observe that the gain margin decreases with increasing v, which is intuitive.

Thus, overall, the proposed DF-AM scheme offers substantial (22% and above) energy efficiency while achieving an appreciable (13% and above) data throughput.

References

[1] M.-S. Alouini and A. J. Goldsmith, "Adaptive modulation over Nakagami fading channels," *Wireless Pers. Commun.*, vol. 13, no. 1, pp. 119-143, 2000.
[2] Q. Liu, S. Zhou, and G. B. Giannakis, "Queuing with adaptive modulation and coding over wireless links: cross-layer analysis and design," *IEEE Trans. Wireless Commun.*, vol. 4, no. 3, pp. 1142–1153, May 2005.
[3] A. Sharma and S. De, "Exploiting fading dynamics along with AMC for energy-efficient transmission over fading channels," *IEEE Commun. Lett*, vol. 15, no. 11, pp. 1218–1220, Nov. 2011.
[4] S. De, A. Sharma, R. Jantti, and D. H. Cavdar, "Channel adaptive stop-and-wait automatic repeat request protocols for short-range wireless links," *IET Commun.*, vol. 6, no. 14, pp. 2128–2137, Sep. 2012.
[5] P. Mukherjee and S. De, "cDIP: Channel-aware dynamic window protocol for energy-efficient IoT communications," *IEEE Internet Things J.*, vol. 5, no. 6, pp. 4474–4485, Dec. 2018.
[6] M. Zorzi, R. R. Rao, and L. B. Milstein, "ARQ error control for fading mobile radio channels," *IEEE Trans. Veh. Technol.*, vol. 46, no. 2, pp. 445–455, May 1997.
[7] A. Goldsmith, *Wireless Communications*. Cambridge Univ. Press, 2005.
[8] S. L. Cotton, "Second-order statistics of κ-μ shadowed fading channels," *IEEE Trans. Veh. Technol.*, vol. 65, no. 10, pp. 8715–8720, Oct. 2016.
[9] W. C. Horrace, "Some results on the multivariate truncated normal distribution," *J. Multivar. Anal.*, vol. 94, no. 1, pp. 209–221, 2005.
[10] A. Genz, "Numerical computation of multivariate normal probabilities," *J. Comput. Graph. Statist.*, vol. 1, no. 2, pp. 141–149, 1992.
[11] (Dec. 2018). *ATZB-900-B0R Datasheet*, Microchip, [Online]. Available: http://ww1.microchip.com/downloads/en/DeviceDoc/doc8227.pdf
[12] T. Rappaport, *Wireless Communications: Principles and Practice*. Upper Saddle River, NJ, USA: Prentice-Hall, 2001.
[13] V. N. Swamy, P. Rigge, G. Ranade, B. Nikolic, and A. Sahai, "Predicting wireless channels for ultra-reliable low-latency sommunications," in *Proc. IEEE Int. Symp. Inf. Theory*, Vail, CO, USA, Jun. 2018, pp. 2609–2613.